Thermodynamics and the glass transition in model energy landscapes

M. Scott Shell* and Pablo G. Debenedetti†
Department of Chemical Engineering, Princeton University, Princeton, New Jersey, 08544, USA
(Received 20 January 2004; published 11 May 2004)

We determine the liquid-state thermodynamics for a model energy landscape corresponding to soft spheres with a mean-field attraction. We consider two approximations, in which the distribution of potential energy minima is either Gaussian or binomial, and for each we calculate the liquid spinodal, binodal, and "effective" glass transition locus. The resulting models provide a unified description of the liquid state across the complete range from low-temperature glassiness to high-temperature instability with respect to the vapor phase.

DOI: 10.1103/PhysRevE.69.051102 PACS number(s): 05.20.Jj, 61.20.Gy, 64.70.Pf, 61.43.Fs

I. INTRODUCTION

The glassy state is ubiquitous in nature; it is also present in many of the plastics and optical devices that we use and an important component of new technologies, from pharmaceuticals to metallic alloys [1,2]. Nonetheless, the fundamental physics underlying the glass transition remains an active area of research [3]. The basic phenomenology of glass formation is familiar: a liquid is supercooled fast enough to bypass crystallization, and eventually reaches a kinetic bottleneck with a sudden albeit continuous transition to a solidlike state [4]. Strictly speaking, this transition is kinetic in nature, and in practice the empirical glass transition temperature depends on the cooling rate employed. It is therefore somewhat surprising that the kinetics of deeply supercooled liquids appear to be tightly linked with their thermodynamics. The relevance of a thermodynamic description of supercooling and vitrification phenomena is a major open question and is the subject of much current research [5–13]. The relationship between kinetics and thermodynamics is exemplified by an equation proposed by Adam and Gibbs almost 40 years ago [14]:

$$\tau = \tau_0 \exp\left(\frac{A}{TS_c}\right), \tag{1}$$

where τ is a characteristic relaxation time, A and τ_0 are constants, T is temperature, and S_c is the so-called configurational entropy of the system. In the original derivation, S_c stems from the number of structural arrangements available to the liquid's constituent molecules. Though work remains to be done in placing the Adam-Gibbs (AG) equation on firmer theoretical ground, the remarkable performance of Eq. (1) for a range of supercooled substances [15] provides empirical support for its use on at least a pragmatic basis.

The energy landscape approach [16,17], which focuses on the topology of a system's potential energy function, has proved useful in investigating the link between kinetics and thermodynamics in supercooled liquids. Important past simulation work has demonstrated the role of the energy landscape in this kinetic-thermodynamic connection [18–23]. In the present work, we take a theoretical approach and examine the implications of a model energy landscape on the phase behavior of the liquid, including the glass transition. This model has been formulated in previous investigations [24,25] and employs a system of spherically symmetric particles, interacting with soft repulsive and mean-field attractive forces. Using this idealized system, we demonstrate the connection between the glass transition and macroscopic thermodynamics in the supercooled region of the phase diagram.

The basis of the energy landscape formalism lies in the statistical characterization of landscape features [17]. Rigorously, a system's energy landscape is its multidimensional potential energy hypersurface as a function of its configurational degrees of freedom. The exponentially numerous local energy minima in an energy landscape, called inherent structures (IS), allow an exact partitioning of configuration space into the basins surrounding them [17]. At a given temperature and density (or pressure), the system samples a degenerate number of inherent structures, $\Omega_{IS}(T,\rho)$, which make an entropic contribution to the total free energy, also called the configurational entropy: $S_c \equiv k_B \ln \Omega_{IS}$. Although without rigorous theoretical justification, one can substitute the landscape-defined configurational entropy into Eq. (1), and the resulting predictions for kinetic constants have been shown in computer simulations to fare quite well [18–21]. Experimentally, on the other hand, the configurational entropy used in the Adam-Gibbs equation is often the excess entropy, that is to say the supercooled liquid's entropy minus that of the stable crystal at the same conditions [15]. The subtraction removes the entropic contribution due to vibrational modes associated with the liquid's configurations. The landscape configurational and excess entropies coincide when the vibrational modes of the liquid and crystal around their respective energy minima are equal.

Much attention has been given to the behavior of S_c in deeply supercooled liquids, with a particular focus on whether or not the configurational entropy reaches zero at finite temperature [24,26–30]. In terms of the landscape, the vanishing of S_c implies that the system has only a single, low-energy amorphous configuration available to it [26]. This fact, coupled with the corresponding behavior of Eq. (1) at such a point, suggests complete structural arrest at $S_c = 0$,

*Email: shell@princeton.edu
†Email: pdebene@princeton.edu

and has since come to be called an ideal glass transition. Contrary to the familiar experimental glass transition, this hypothetical phenomenon is thermodynamic, occurring at a well-defined temperature T_{IG}. The ideal glass transition has emerged as an interesting theoretical construct in spin glass [31,32], liquid [33–35], and protein [36,37] models, but owing to the antecedence of the real, kinetic glass transition, it has never been experimentally observed.

The ideal glass transition is often associated with the so-called Kauzmann point, T_K, at which the excess entropy reaches zero [26,38]. Walter Kauzmann [39] observed that for a number of substances the entropy of the supercooled liquid decreases quite rapidly upon cooling and, with reasonable extrapolation, appears to become less than that of the stable crystal at a finite temperature. If this trend were to continue to absolute zero, the liquid would attain a negative entropy, in violation of the third law of thermodynamics. Experimentally the glass transition intervenes above T_K, avoiding this supposed catastrophe [2], but the unsettling implications of the behavior leading up to the Kauzmann point have led to the (perhaps unfounded) belief that an ideal glass transition exists near T_K to ensure thermodynamic consistency. It is now understood that Kauzmann points can and do exist in several substances without an accompanying ideal glass transition or any violation of the third law [29]. On the other hand, theoretical considerations argue against the possibility of vanishing configurational entropy at finite temperature [26], making the ideal glass transition an unrealistic feature of liquids.

We employ a model energy landscape [24,25] and investigate both its kinetic and thermodynamic properties. The model entails representative parameters which approximate Lennard-Jones-type systems, and gives a realistic description of simple liquids at low temperatures. We examine two variations on this system, in which it exhibits or avoids an ideal glass transition, and extract the corresponding phase diagrams for the liquid state. Motivated by the AG relationship, we also calculate an effective, "laboratory" glass transition locus and examine the kinetic behavior leading up to T_G. Section II reviews the energy landscape formalism and the argument against the existence of the glass transition. The model and its predictions are presented in Sec. III, and the generality and implications of these results are discussed in Sec. IV.

II. THE ENERGY LANDSCAPE AND IDEAL GLASSES

In principle, a system's energy landscape, given by its potential energy function, contains the complete information on its thermodynamic and kinetic behavior. In practice, however, the overwhelming complexity of this hypersurface necessitates a statistical characterization rather than an exact enumeration for all except the smallest systems [40,41]. It has been shown that the equilibrium free energy of a system relates directly to statistical properties of its landscape. In the case of a single component, the free energy is given by [17]

$$a(\rho,T) = \phi^* - k_B T\sigma(\phi^*,\rho) + a_{\mathrm{vib}}(T,\phi^*,\rho), \tag{2}$$

where a is the per-particle Helmholtz free energy, ρ is the density, k_B is Boltzmann's constant, and $\phi^*(T,\rho)$, which minimizes this expression, is the average inherent structure energy sampled by the system. The functions σ and a_{vib} make the rigorous connection with landscape properties, and are termed the basin enumeration function and vibrational free energy, respectively. In particular, the quantity $S_c \equiv Nk_B\sigma(\phi^*,\rho)$ is the total configurational entropy. For a system of N structureless particles, these functions are defined by

$$d\Omega_{\mathrm{IS}}(\phi) = C\,\exp[N\sigma]d\phi, \tag{3a}$$

$$e^{-\beta N a_{\mathrm{vib}}} = \Lambda^{-dN}\left\langle \int_{\Gamma_k} e^{-\beta[U(\mathbf{r}^N)-U_k]}d\mathbf{r}^N \right\rangle_{\phi}, \tag{3b}$$

where $\beta = 1/k_BT$, d is dimensionality, Λ is the thermal de Broglie wavelength, U is the potential energy, and $\mathbf{r}^N$ are the atomic coordinates. Here, the basin enumeration function relates directly to the energy distribution of inherent structures: $d\Omega_{\mathrm{IS}}(\phi)$ gives the number of minima with per-particle energy $\phi \pm d\phi/2$, and C is a constant which has no bearing on thermodynamics. For the supercooled liquid and glass, one must exclude any crystalline configurations from the counting embodied in Ω_{IS}. Furthermore, $a_{\mathrm{vib}}(T,\phi,\rho)$ is the average free energy of basins of depth ϕ; in Eq. (3b), the average is restricted to minima of energy ϕ and the integral for a particular minimum k, of energy U_k, is performed over its basin's configuration space Γ_k.

Careful attention must be paid to the determination of ϕ^*, the equilibrium inherent structure energy [24]. The particular issue at hand is whether or not the system reaches its minimum amorphous energy, $\phi_{\mathrm{min}}(\rho)$, at finite temperature. Presumably only a single amorphous configuration is available at this energy, which implies a simultaneous vanishing of the configurational entropy; in other words, $\sigma(\phi_{\mathrm{min}})=0$. If reached at a finite temperature, this point represents an ideal glass transition. At lower temperatures, the system remains confined to this lowest-energy configuration, with $\phi^*=\phi_{\mathrm{min}}$ and $\sigma=0$. In mathematical terms, the behavior of ϕ^* is given by

$$\frac{\partial\sigma(\phi^*,\rho)}{\partial\phi} = \beta\left[1 + \frac{\partial a_{\mathrm{vib}}(T,\phi^*,\rho)}{\partial\phi}\right] \quad \text{for } T > T_{\mathrm{IG}}(\rho),$$

$$\phi^* = \phi_{\mathrm{min}}(\rho) \quad \text{for } T \leqslant T_{\mathrm{IG}}(\rho), \tag{4}$$

where the ideal glass transition locus $T_{\mathrm{IG}}(\rho)$ is determined from

$$\frac{\partial\sigma(\phi_{\mathrm{min}},\rho)}{\partial\phi} = \beta_{\mathrm{IG}}\left[1 + \frac{\partial a_{\mathrm{vib}}(T_{\mathrm{IG}},\phi_{\mathrm{min}},\rho)}{\partial\phi}\right]. \tag{5}$$

From this expression, one can see that if the limiting slope of the basin enumeration function at ϕ_{min} is infinite, corresponding to the left-hand side of Eq. (5), no positive-temperature ideal glass transition exists. (We should note that a_{vib} is typically weakly ϕ-dependent at low temperatures, and no singular dependence is expected.) Consequently, the existence of an ideal glass transition is tied to the behavior of the amorphous basin enumeration function at its minimum energy. A Kauzmann point, on the other

hand, additionally depends on the behavior of the crystal phase. Since the crystal always exists in a unique basin and its configurational entropy is therefore rigorously zero [42], the location of a Kauzmann point requires one to consider the vibrational entropies, $s_v \equiv -\partial a_{vib}/\partial T$, of both phases in addition to the liquid configurational entropy. Due to this involvement of the vibrational entropies, a Kauzmann point can occur completely independent of an ideal glass transition [29].

A simple consideration of the local nature of microscopic interactions disputes the possibility of an ideal glass transition at finite T, namely, by demonstrating that the slope of σ with respect to ϕ must be infinite at ϕ_{min} [26,43]. A rough outline of the argument is as follows: consider a large system of N particles which is macroscopic in size, and let $\Omega_{IS}(N,\Phi_{min}+\Delta\Phi)$ be the degeneracy of the second energy level of minima, the ground state being nondegenerate. If we replicate the system n times, the boundary interactions between each copy are to a good degree negligible due to their macroscopic size, and so an energy minimum in the composite system is given by a combination of minima among the individual subsystems. This gives a lower bound for Ω_{IS} for the overall system:

$$\Omega_{IS}(nN, n\Phi_{min} + m\Delta\Phi) \geqslant \binom{n}{m} \Omega_{IS}(N, \Phi_{min} + \Delta\Phi)^m, \quad (6)$$

where m is the number of subsystems in the second energy level. By taking the logarithm of this expression and dividing by the total number of particles nN, one obtains the leading behavior of the basin enumeration function:

$$\sigma(\phi_{min} + y\Delta\phi) \geqslant -(y \ln y)/N + \text{additional terms}, \quad (7)$$

where $y \equiv m/n$ and Stirling's approximation has been employed. In the limit of a very large number of replicas (i.e., at the thermodynamic limit $n \to \infty$), y is essentially a continuous variable. Then, the slope of the basin enumeration function at its minimum energy is related to the y derivative of Eq. (7) evaluated at $y=0$. Because this derivative diverges, the system only reaches its ground state at zero temperature, and hence no ideal glass transition exists.

The logarithmic divergence of the slope of σ at ϕ_{min}, therefore, should be a feature of any model basin enumeration function which aims to capture the low-temperature behavior of liquids. However, simpler functional forms are often easier to implement, and in this sense, the Gaussian expression has been particularly well studied in the energy landscape context [43–47]:

$$\sigma(\phi,\rho) = \sigma_\infty(\rho)\left[1 - \left(\frac{\phi - \phi_\infty(\rho)}{\phi_\infty(\rho) - \phi_{min}(\rho)}\right)^2\right], \quad (8)$$

where σ_∞ and ϕ_∞ are the maximum value of σ and its corresponding energy. Equation (8) gives rise to a Gaussian energy distribution of inherent structures, but owing to its behavior at the minimum energy ϕ_{min}, also possesses an ideal glass transition. That is, the distribution is actually truncated at ϕ_{min}, where the configurational entropy vanishes, and its slope at this point gives the ideal glass transition locus. The Gaussian form is often thought to emerge due to the central limit theorem, although a careful consideration of this line of thought shows that non-Gaussian corrections can remain important [48]. It is perhaps more appropriate to think of Eq. (8) as an expansion to second order.

Motivated by the form of the Gaussian landscape, one might consider parameterizing the density dependence of basin enumeration functions in the following manner [24,43]:

$$\sigma(\phi,\rho) = \sigma_\infty(\rho) f[u] \quad \text{with } u \equiv \frac{\phi - \phi_\infty(\rho)}{\phi_\infty(\rho) - \phi_{min}(\rho)}, \quad (9)$$

where u is the normalized inherent structure energy, equal to -1 at ϕ_{min}, and f is the dimensionless form of the basin enumeration function, varying between zero and one. In the Gaussian landscape, one simply has $f[u]=1-u^2$. Though the assumption of a density-independent functionality $f[u]$ cannot be rigorously true for all systems, it serves as a useful theoretical starting point and simplifies the analysis of simulation data.

Recently an additional model basin enumeration function has been suggested, the so-called logarithmic landscape [43], which is closely related to the "bond-lattice" model of Angell and co-workers [49–51]. Essentially a binomial distribution, the logarithmic model envisions a liquid's inherent structures as being composed of an extensive number of identical elementary structures, each of which exists in either a high or low-energy state. It gives rise to the following functional form for σ, expressed in dimensionless form according to Eq. (9):

$$f[u] = 1 - \frac{1}{\ln(4)}[(1-u)\ln(1-u) + (1+u)\ln(1+u)]. \quad (10)$$

The logarithmic landscape gives exactly the leading low-energy behavior anticipated in Eq. (7), and consequently, does not possess an ideal glass transition. However, its binary description is a much simplified portrayal of the way in which real inherent structures arise, and hence it alone does not necessarily give a quantitatively accurate picture. It has been shown that by "mixing" the logarithmic and Gaussian landscapes through a linear combination of their $f[u]$, one can always extrapolate high-temperature data in a way that predicts an apparent ideal glass transition, although it is narrowly avoided upon closer approach [43]. The situation for the purely Gaussian and logarithmic cases is depicted in Fig. 1: by extrapolating the temperature dependence of the configurational entropy in the logarithmic landscape, one might be tempted to predict an ideal glass transition around reduced temperature 0.25.

III. MODEL LANDSCAPES

A. Model description

In order to explore the effects of the Gaussian and logarithmic landscapes on the full liquid-state phase diagram, the density dependence of the parameters ϕ_{min}, ϕ_∞, and σ_∞ is required. Here, we consider the case of soft spheres interact-

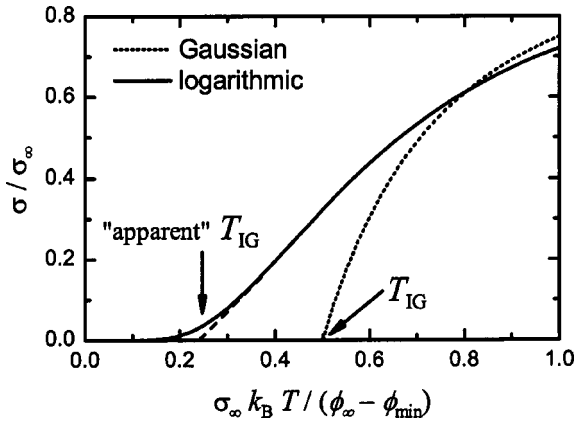

FIG. 1. Evolution of the normalized configurational entropy as a function of dimensionless temperature for the Gaussian and logarithmic landscapes. In the Gaussian case, a rigorous ideal glass transition exists at reduced temperature 0.5. A modest extrapolation might predict an apparent ideal glass transition for the logarithmic landscape, although it is never realized at finite temperature. Here, the vibrational free energy has been assumed to be independent of basin depth.

ing through an inverse power repulsion with an additional mean-field attraction. At a given density, the potential energy for this soft-sphere mean-field (SSMF) system is given by

$$U(\mathbf{r}^N,\rho) = \sum_{i<j} \epsilon(\sigma/r_{ij})^n - Na\rho, \tag{11}$$

where ϵ and σ are the soft-sphere energy and length scales, n is the repulsive exponent, and a is the attractive mean-field term. This system is appropriate to simple liquids whose molecules interact in a spherically symmetric fashion, and its energy landscape has been investigated in some detail [24,25,29,52–54]. The important feature of the SSMF model is that the functional forms in density of all its landscape parameters are known explicitly [24]:

$$\sigma_\infty(\rho) = \sigma_\infty, \tag{12a}$$

$$\phi_\infty(\rho) = \gamma_\infty \rho^{n/3} - a\rho, \tag{12b}$$

$$\phi_{\min}(\rho) = \gamma_{\min}\rho^{n/3} - a\rho, \tag{12c}$$

where $\gamma_{\min}$ and γ_∞ are constants corresponding to configurations at the minimum energy and maximum configurational entropy of the basin enumeration function, respectively. The general expression for γ, which is averaged over the respective configurations to produce $\gamma_{\min}$ and γ_∞, is given by

$$\gamma(\mathbf{r}^N) \equiv \epsilon\sigma^3 \frac{1}{N^{1+n/3}} \sum_{i<j} \left(\frac{r_{ij}}{V^{1/3}} \right)^{-n}. \tag{13}$$

Combined with the Gaussian or logarithmic landscape, the expressions in Eqs. (12a)–(12c) enable an explicit evaluation of the basin enumeration function in both energy and density.

The remaining ingredient required for the evaluation of the free energy in Eq. (2) is the functional form of the vibrational free energy. For this, we employ the Einstein approximation, assuming each basin to be parabolic in shape around its minimum and characterized by a single frequency (or curvature). This approximation is valid at very low temperatures, where the system spends much of its time near minima with negligible anharmonic contributions. The resulting expression is [24]

$$a_{\text{vib}}(T,\phi,\rho) = 3k_B T \ln(\Theta_E/T), \tag{14}$$

where the factor of 3 stems from the dimensionality and Θ_E is used as the amorphous equivalent of the Einstein temperature. We further assume for our calculations that a_{vib} (and hence also Θ_E) is independent of ϕ. This assumption is increasingly accurate as one approaches absolute zero, although simulation results indicate a nonzero, albeit weak ϕ dependence at finite temperatures for a number of substances [19,46,47]. It is nonetheless somewhat comforting that an expansion of a_{vib} to linear order in ϕ does not change the results presented below except to scale the temperature [43].

In summary, the free energy of the SSMF model relies on a total of six parameters: n, σ_∞, $\gamma_{\min}$, γ_∞, a, and Θ_E. We have chosen representative values which loosely approximate the behavior of the Lennard-Jones (LJ) liquid, all of which are expressed here in reduced units. We set $n=12$ and use $\sigma_\infty = 1.0$ based on previous estimates [19,55]. Reference [56] has suggested an Einstein frequency of roughly 2.0 for LJ liquid inherent structures; therefore, we use $k\Theta_E = 2.0$. We note that Θ_E affects only our vapor-liquid binodal calculations, and those results are quite insensitive to its precise value. Finally, the three parameters $\gamma_{\min}=3.77$, $\gamma_\infty=4.64$, and $a=16.5$ are chosen by fitting the equation of state predicted by Eq. (2) to simulation data [24].

B. Phase behavior

The overall liquid-state phase behavior of the SSMF model in both the Gaussian and logarithmic landscape approximations is depicted in Fig. 2. Below we detail the methods used for these calculations, but for clarity we first examine a few thermodynamic paths in the phase diagrams. First, consider the case when the density is gradually decreased at constant temperature. Starting in the liquid regime at $\rho=0.9$ and $T=0.7$, upon decreasing the density one first passes the binodal line, which would normally mark the onset of phase coexistence with the appearance of an infinitesimal amount of vapor. If, however, the liquid is maintained in a metastable state, it can be further decompressed until it ultimately becomes unstable at the liquid spinodal. Just prior to reaching this point, however, the inherent structures are found to be unstable at their associated spinodal; the effect of vibrational motions around a basin therefore enables the system to withstand the greater decompression at the densities between the two spinodals. Note that at fixed temperature the density is higher at the inherent structure spinodal than at the liquid spinodal, but the tension is smaller (pressure less negative) at the liquid spinodal.

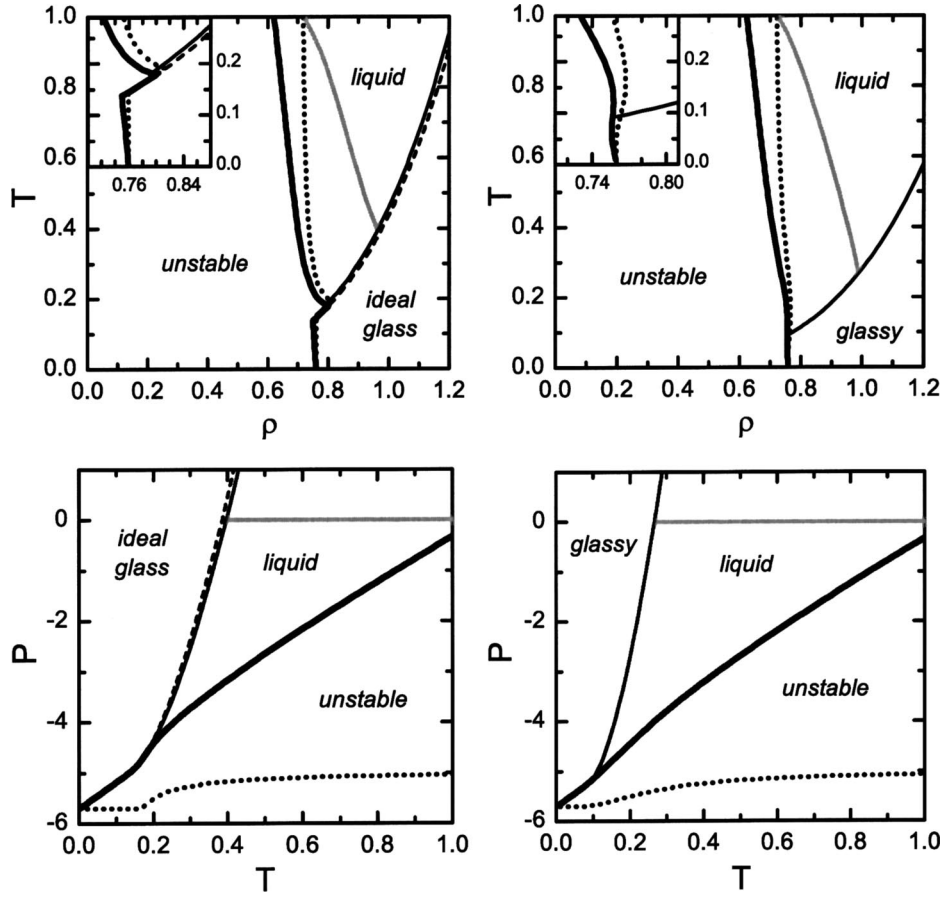

FIG. 2. Phase behavior in the T-ρ (top) and P-T (bottom) planes of the SSME model with Gaussian (left) and logarithmic (right) landscapes. The heavy solid line is the liquid spinodal at which the density derivative of the pressure vanishes; the dotted line is the corresponding spinodal for the inherent-structure contribution to the pressure. The thin solid line is the approximated glass transition locus, at which $S_c=0.1(S_c)_{\max}$. The dashed line is the ideal glass transition, at which $S_c=0$. The gray line is the liquid binodal, calculated in conjunction with the ideal gas free energy. The insets detail the region where the spinodal and glass transition lines intersect.

If the liquid is cooled at high enough density, it enters a glassy phase; in the Gaussian case, this is an ideal glass where the configurational entropy is rigorously zero, whereas in the logarithmic model, the glassy domain is characterized by a small configurational entropy. The glass transition can also be reached by compressing the liquid at a fixed temperature to sufficiently high density. At very low temperatures, however, the system cannot exist in the normal (fluid) liquid state and must either be glassy or unstable. At these low temperatures and upon isotropically stretching the glass, one eventually reaches instability directly, at which point the system presumably begins to sublimate as coexistence between a gas and glass phase is established. If this decompression were to continue, the amount of the vapor would increase at the expense of the glass.

If the liquid is cooled at a lower density, for example $\rho=0.75$, it instead encounters the inherent-structure and total spinodals upon cooling, in that respective order, and hence becomes unstable with respect to the vapor before vitrifying. In the Gaussian case around $\rho=0.78$, a particularly interesting possibility is that the spinodals can also be reached by heating when the starting point is a much lower temperature (e.g., $T=0.1$). The discontinuous zigzag character of the Gaussian spinodal in the T-ρ plane, which causes this unusual behavior, is due to the existence of the ideal glass transition and associated discontinuities (discussed below). However, the logarithmic case also possesses nonmonatomic spinodal character, although it is much smoother and occurs over less than half the density range of the Gaussian zig-zag feature.

The pressure of the SSMF liquid is given, as usual, by $\rho^2(\partial a/\partial\rho)_T$, with a as per Eq. (2). In the landscape formalism, the resulting expression can be further subdivided into inherent structure and vibrational components [24,57]:

$$P_{\rm IS}=\rho^2\left[\frac{d\phi_\infty}{d\rho}+u^*\frac{d(\phi_\infty-\phi_{\min})}{d\rho}\right] \quad \text{for } T>T_{\rm IG},$$

$$P_{\rm IS}=\rho^2\frac{d\phi_{\min}}{d\rho} \quad \text{for } T\leqslant T_{\rm IG}, \tag{15a}$$

$$P_{\rm vib}=\rho^2\frac{\partial a_{\rm vib}}{\partial\rho}=\frac{n+2}{2}\rho k_BT. \tag{15b}$$

Here, u^* is the equilibrium value of u, defined by Eqs. (4) and (9). The total pressure is simply $P=P_{\rm IS}+P_{\rm vib}$. It is

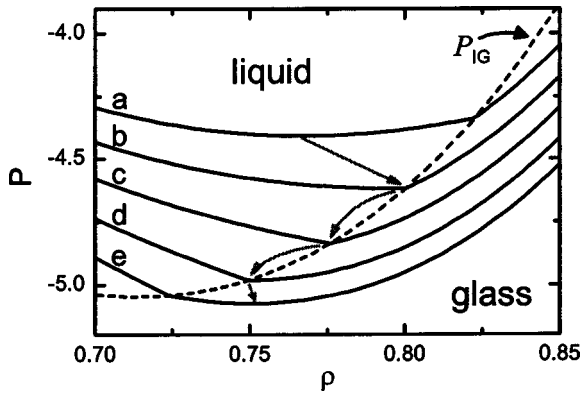

FIG. 3. Evolution of the pressure across the ideal glass transition, where the isotherms (a)–(e) correspond to $T=0.20$, 0.18, 0.16, 0.14, and 0.12, respectively. Along (a), the minimum in pressure occurs in the liquid side; likewise for (e), the minimum occurs in the ideal glass regime. As one cools from (a) to (b), the minimum moves to higher densities and eventually meets the ideal glass transition locus. Then, upon further cooling the pressure minimum moves with the ideal glass locus to lower densities until the limiting temperature at (d), where the portion of the isotherm on the glass side develops a minimum. At lower temperatures, then, the minimum always occurs in the glass regime.

straightforwared to see that at T_{IG}, where the system is in its minimum energy configurationand $u^*=-1$, the two expressions in Eq. (15a) yield the same pressure. Therefore, the pressure is continuous across the ideal glass transition, although its derivative is not and in particular, pressure-versus-density isotherms exhibit a discontinuous slope at this point [24,58].

The liquid spinodal represents the point of limiting stability, beyond which the liquid can no longer exist as a homogeneous phase. The thermodynamic condition at the spinodal which we use for its calculation is

$$\left(\frac{\partial P}{\partial \rho}\right)_T = 0. \tag{16}$$

The border of the unstable region in the SSMF model is shown in the phase diagrams of Fig. 2. The Gaussian case possesses the interesting feature that this line intersects and becomes identical to the ideal glass line for the small temperature range of $T=0.14-0.18$. This feature arises because in this temperature range the slope discontinuity of isotherms in the (P,ρ) plane, associated with the ideal glass transition, also entails a change of sign. This is shown in Fig. 3, which displays several isotherms spanning the temperature range $T=0.14-0.18$. The slope discontinuity propagates to progressively lower densities as the temperature is lowered.

The effects of the ideal-glass discontinuities on the spinodal require special attention. While it is true that the thick spinodal-labelled line in the phase diagrams of Fig. 2. traces a border between stable and unstable regions, this locus does not rigorously adhere to the instability condition in Eq. (16) along the ideal glass transition, where instead the density derivative of the pressure changes sign discontinuously. That is, the loci defined by Eq. (16) in both the liquid and ideal glass regimes do not meet in the T-ρ plane, and it would appear that no true spinodal exists in the temperature range $T=0.14-0.18$. At these intermediate temperatures, a cusp (slope discontinuity) preempts the attainment of the minimum. Isothermal decompression of the ideal glass leads to an unstable liquid without an intervening infinite compressibility condition $(\partial P/\partial\rho=0)$. This peculiarity is a direct consequence of the truncation of the Gaussian distribution at the minimum amorphous energy. To examine this behavior in more detail, we consider the Gaussian landscape as a limiting discontinuous form of a family of continuous basin enumeration functions. In particular, we are motivated by the logarithmic correction discussed in Sec. II to examine the family of basin enumeration functions which interpolate smoothly between the logarithmic and Gaussian models [43]:

$$f[u] = (1-x)f_{\text{Gaussian}}[u] + xf_{\text{logarithmic}}[u], \tag{17}$$

where x is the interpolation variable ranging from zero (purely Gaussian) to one (purely logarithmic). Due to the form of the logarithmic basin enumeration function, the "mixed" landscape will never possess an ideal glass transition for a nonzero value of x. Therefore, none of the aforementioned $dP/d\rho$ slope discontinuities arise for finite x, and a continuous spinodal can always be extracted. In taking the limit $x\to 0$, the pressure-versus-density plots develop a progressively sharper cusp whose slope is rigorously discontinuous at $x=0$. Simultaneously as x proceeds to zero, the liquid spinodal in this family of landscapes gradually approaches the so-labelled line in Fig. 2, in which it traces the ideal glass transition between the liquid and glass regimes. In other words, a portion of the region defined by Eq. (16) collapses onto the ideal glass locus as we take this limit.

Since the inherent-structure pressure is known independently of the total, it is also possible to define an inherent-structure spinodal by replacing P with P_{IS} in Eq. (16) [44]. At a given temperature, this spinodal refers to the minimum inherent-structure pressure and corresponding density. A number of simulation studies suggest that the P_{IS} spinodal has an interesting connection to instability, microscopic heterogeneity, and ultimate mechanical strength [44,46,53,59–62]. The calculations for the inherent structure spinodal are reported in the phase diagrams. Similar to the case for the total pressure, a slope discontinuity also exists in P_{IS} in the Gaussian case, which causes the border between inherent-structure stability and instability to trace the ideal glass locus for a similar (but distinct) temperature range.

In Fig. 2, we also show the liquid side of the vapor-liquid coexistence curve. We determine this locus by equating the chemical potential in the SSMF model with that of an ideal gas:

$$a(T,\rho) + P(T,\rho)/\rho = \mu_{\text{ideal gas}}(T,P), \tag{18}$$

where the left-hand side of this equation corresponds to the liquid phase. At a given temperature, ρ gives the total pressure (from the liquid side) and is iterated until this equation converges. Though our use of the ideal gas model becomes unreliable at high temperatures, it gives at least a qualitative

description of the liquid equilibrium behavior for the low temperatures examined here.

C. Glass transition locus

Of the two basin enumeration functions examined, only the Gaussian form possesses an ideal glass transition. Using Eq. (5), the T_{IG} locus in the SSMF model with a Gaussian landscape is given by

$$T_{\mathrm{IG}} = \frac{\phi_\infty(\rho) - \phi_{\min}(\rho)}{2k_B\sigma_\infty}. \tag{19}$$

The ideal glass transition represents the point of structural arrest in a thermodynamic sense, but it is also desirable to identify an effective laboratory glass transition at which the characteristic timescales of the supercooled liquid grow to laboratory magnitudes. The Adam-Gibbs equation offers the possibility of such a calculation; if one associates a critical timescale τ with the glass transition [1], T_{G} can be identified as the thermodynamic locus yielding the corresponding valueof the exponent in Eq. (1). For the current model, we take a simpler approach and locate the boundary in the phase diagram for which the configurational entropy is 10% of its maximum value, given by

$$\frac{\sigma(\phi^*,\rho)}{\sigma_\infty} = f[u^*] = 0.1, \tag{20}$$

where ϕ^* and u^* are functions of temperature and density. The choice of this line as an effective glass transition is an approximation to the AG equation, which instead suggests that the quantity $T_{\mathrm{G}}S_{\mathrm{c}}(T_{\mathrm{G}})$ is constant at fixed τ. We have also investigated the line of constant TS_{c} which intersects the constant entropy locus defined by Eq. (20) at $\rho=1.0$ (results not shown); these two curves deviate on average by only 3% in temperature for the Gaussian and 10% for the logarithmic case, when viewed as a function of density. Our use of the 10% entropy condition for the prediction of the glass transition is motivated by convenience, since it does not require the (here unknown) constants in the AG equation. Furthermore, we note that changing this requirement by a few percent causes only very minor shifts in the calculated glass loci displayed in Fig. 2.

Of particular interest are the behavior of kinetic coefficients as the glass transition is approached. Based on the Adam-Gibbs equation (1), the logarithm of quantities such as diffusivity and viscosity should be proportional to $(TS_c)^{-1}$:

$$\ln\left(\frac{\tau}{\tau_0}\right) = \frac{A}{TS_{\mathrm{c}}} \tag{21}$$

Therefore, a plot of the right hand side of this equation as a function of temperature is, within the AG approximation, the relevant measure of kinetics in terms of the energy landscape [8]. This is depicted in Fig. 4, where the axes have been normalized to their value at the glass transition temperature as effectively defined by the 10% entropy condition. It should also be noted that these results are independent of the choice of $\phi_{\min}$, ϕ_∞, and σ_∞, due to the way this isochoric data is normalized; therefore, this measure of fragility

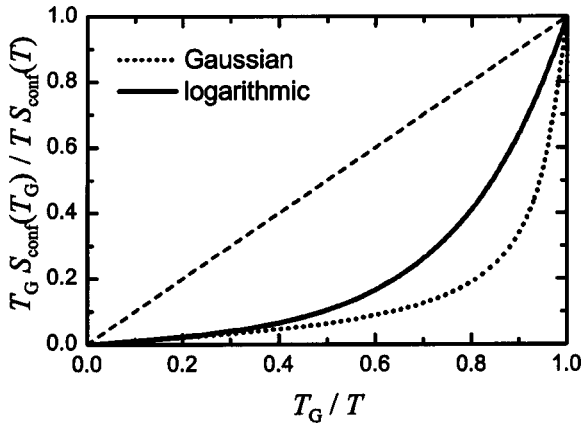

FIG. 4. Fragility plot for the Gaussian and logarithmic landscapes. In the Adam-Gibbs approximation, the quantity $(TS_{\mathrm{c}})^{-1}$ has a linear relationship with the logarithm of a characteristic molecular relaxation time. Here this quantity is shown as a function of inverse temperature, and Arrhenius behavior corresponds to a straight line in the plot. Each of the axes has been normalized to unity at the glass transition.

is independent of density for the models considered. In Fig. 4, both the Gaussian and logarithmic landscapes exhibit so-called "fragile" behavior [63], deviating notably from straight-line Arrhenius form. The logarithmic case appears less fragile, which is compatible with the fact that its basin enumeration function has a smaller absolute value of the curvature at its peak. However, the fragility of both landscapes can be tuned by varying the glass transition criterion.

It is important in interpreting Fig. 4 to keep in mind the approximations made in this work. Aside from possible deviations from AG behavior, the assumption that the vibrational free energy is independent of basin depth breaks down at higher temperatures. This effect will certainly modify the behavior of the curves, and so the possibility exists that only the predictions towards the very right of Fig. 4 are accurate, and in this small temperature range, both curves might appear linear. Furthermore, we have used a simplified criterion for the glass transition temperature, involving the configurational entropy alone and leaving a more detailed analysis to future work. Even the conceptual determination of fragility from landscape models has been the subject of some debate [8,19]; we refer the interested reader to the more thorough discussion in Ref. [64] (see p. 11).

IV. DISCUSSION AND CONCLUSIONS

One can think of the liquid state as bounded by two limits: at fixed temperature, mechanical instability gives rise to a low-density extremum and kinetic sluggishness creates a glassy limit at high density [58]. The energy landscape viewpoint offers a theoretical framework for the treatment of both of these constraints. While the spinodal emerges directly from the thermodynamics of the metastable liquid, it is the identification of the configurational contribution to the entropy, in conjunction with the Adam-Gibbs equation, that enables the landscape's connection with dynamics. The validity

of the AG relationship has not yet been fully established from the landscape-theoretic viewpoint, and so its consideration in the present work must be justified by the empirical evidence which has been found for a number of systems [18–21]. Nonetheless, the configurational entropy, related to the number of distinct configurations that a system can explore, intuitively seems an important ingredient in kinetic behavior, motivating its study in this context.

The phase diagrams we have presented in Fig. 2 utilize a model energy landscape for the calculation of both the liquid spinodal and effective glass transition. Our model is strictly an approximation to real liquids, representing one of the simplest constructs amenable to energy landscape analysis. One might make an analogy with the van der Waals equation in that the mean-field attraction is closely related to the low-density side of the liquid phase (and spinodal), while the repulsive forces affect the behavior at high densities. It is interesting to note that hard repulsive forces, which are approximated by an excluded volume in van der Waals theory, require special treatment in a landscape description [52].

On first viewing, the qualitative similarity between the Gaussian and logarithmic predictions is quite remarkable. If these two forms represent realistic approximations for the actual soft-sphere basin enumeration function, then its true behavior might be considered a modest interpolation of the two; the effects of mixing the two landscapes has been explored in some detail [43]. It is important here that the same parameter values were employed for both cases. The possibility exists that the phase diagrams might exhibit even greater similarity if the two forms are allowed differing parameter sets. From a kinetic point of view, the Gaussian landscape appears more fragile than the logarithmic case, within the limits of the Adam-Gibbs equation, the approximation that a_{vib} is not a function of ϕ, and our heuristic glass transition criterion. An important future study should consider the behavior when each of these approximations is relaxed.

For both versions of the model, the calculated phase diagram indicates the existence of lower temperature and pressure bounds for the liquid. At temperatures below approximately 0.18 and 0.09 for the Gaussian and logarithmic cases, respectively, the liquid state is always glassy and the spinodal becomes the limit of mechanical stability of the glass. This is in agreement with the findings in Ref. [58], in which a similar bound was calculated for a binary Lennard-Jones glass former. The intersection of the spinodal and glass transition loci therefore appears to define an important point in the phase diagram of supercooled liquids. The present mean-field model does not take into account the kinetic aspects of instability, which would also suggest an intriguing convergence of slow, glassy dynamics and rapid nucleation at this point. This matter will be the subject of future research.

In the Gaussian landscape, the ideal glass transition differs almost negligibly from its effective T_{G} counterpart. This result suggests that, regardless of its existence, the ideal version may be a useful theoretical extrapolation in that its locationis not too distant from the onset of very sluggish behavior. On a different note, however, the ideal glass transition imparts an pronounced "kink" in the T-ρ spinodal. This feature arises from the existence of separate liquid and glass pressure branches which meet with a slope discontinuity. While this zig-zag appearance of the spinodal seems unrealistic, smoothed traces of this behavior still exist in the logarithmic case.

Finally, we comment on the behavior of the inherent structure spinodal predicted by the model. In particular, for simple systems, it has been found that the minimum in P_{IS} and corresponding density vary little with temperature [44], that is, the IS spinodal in these systems is driven largely by volume effects. The same is true of the SSMF model; in either the Gaussian or logarithmic approximation, the density and pressure of the IS spinodal vary by only $5-15\%$ over the temperature range investigated. Since the total and IS spinodals converge at absolute zero, the current work suggests that the latter, measured at finite temperature, serves as a good approximation to the $T=0$ spinodal limit [53]. However, we note that this is not likely the case for complex systems such as water, in which the density dependence of landscape properties is more intricate [47,59].

The present work underscores the importance of the energy landscape in the understanding of supercooled liquids and their glasses. Through an exact expression for thermodynamics and the approximate Adam-Gibbs relationship for kinetic behavior, key measures of a landscape are straightforwardly related to its bulk thermophysical properties. Still, the connection between a system's molecular interactions and the statistical properties of its highly dimensional potential energy surface is extremely difficult to elucidate analytically, with the exception of a very small number of special systems like the soft-sphere mean-field model examined here. As a result, most landscape investigations are computational in nature. Much work remains to be done in establishing simple, perhaps approximate, expressions for the effects of molecular interactions on landscape properties such as basin curvature and shape of the inherent-structure distribution [65].

ACKNOWLEDGMENTS

This work is an offspring of a collaboration with E. La Nave and F. Sciortino, whom we thank for useful discussions. We also thank A. Panagiotopoulos for helpful comments. Finally, we gratefully acknowledge the support of the Fannie and John Hertz Foundation and of the Department of Energy, Division of Chemical Sciences, Geosciences, and Biosciences, Office of Basic Energy Science (Grant No. DE-FG02-87ER13714).

[1] C. A. Angell, Science **267**, 1924 (1995).
[2] P. G. Debenedetti and F. H. Stillinger, Nature (London) **410**, 259 (2001).
[3] Special issue of J. Phys.: Condens. Matter **15**, S737–S1290 (2003).
[4] P. G. Debenedetti, *Metastable Liquids: Concepts and Principles* (Princeton University Press, Princeton, N.J., 1996).
[5] F. H. Stillinger, Science **267**, 1935 (1995).
[6] T. M. Nieuwenhuizen, Phys. Rev. Lett. **80**, 5580 (1998).
[7] S. Sastry, P. G. Debenedetti, and F. H. Stillinger, Nature (London) **393**, 554 (1998).
[8] R. J. Speedy, J. Phys. Chem. B **103**, 4060 (1999).
[9] X. Y. Xia and P. G. Wolynes, Proc. Natl. Acad. Sci. U.S.A. **97**, 2990 (2000).
[10] L. M. Martinez and C. A. Angell, Nature (London) **410**, 663 (2001).
[11] U. Mohanty, N. Craig, and J. T. Fourkas, J. Chem. Phys. **114**, 10577 (2001).
[12] F. W. Starr, C. A. Angell, E. La Nave, S. Sastry, A. Scala, F. Sciortino, and H. E. Stanley, Biophys. Chem. **105**, 573 (2003).
[13] M. P. Eastwood and P. G. Wolynes, Europhys. Lett. **60**, 587 (2002).
[14] G. Adam and J. H. Gibbs, J. Chem. Phys. **43**, 139 (1965).
[15] R. Richert and C. A. Angell, J. Chem. Phys. **108**, 9016 (1998).
[16] M. Goldstein, J. Chem. Phys. **51**, 3728 (1969).
[17] F. H. Stillinger and T. A. Weber, Phys. Rev. A **25**, 978 (1982).
[18] A. Scala, F. W. Starr, E. La Nave, F. Sciortino, and H. E. Stanley, Nature (London) **406**, 166 (2000).
[19] S. Sastry, Nature (London) **409**, 164 (2001).
[20] I. Saika-Voivod, P. H. Poole, and F. Sciortino, Nature (London) **412**, 514 (2001).
[21] S. Mossa, E. La Nave, H. E. Stanley, C. Donati, F. Sciortino, and P. Tartaglia, Phys. Rev. E **65**, 041205 (2002).
[22] L. Angelani, R. Di Leonardo, G. Ruocco, A. Scala, and F. Sciortino, Phys. Rev. Lett. **85**, 5356 (2000).
[23] K. Broderix, K. K. Bhattacharya, A. Cavagna, A. Zippelius, and I. Giardina, Phys. Rev. Lett. **85**, 5360 (2000).
[24] M. S. Shell, P. G. Debenedetti, E. La Nave, and F. Sciortino, J. Chem. Phys. **118**, 8821 (2003).
[25] R. J. Speedy, J. Phys.: Condens. Matter **15**, S1243 (2003).
[26] F. H. Stillinger, J. Chem. Phys. **88**, 7818 (1988).
[27] K. Binder, J. Baschnagel, and W. Paul, Prog. Polym. Sci. **28**, 115 (2003).
[28] F. Sciortino, W. Kob, and P. Tartaglia, J. Phys.: Condens. Matter **12**, 6525 (2000).
[29] F. H. Stillinger, P. G. Debenedetti, and T. M. Truskett, J. Phys. Chem. B **105**, 11809 (2001).
[30] R. J. Speedy, Biophys. Chem. **105**, 411 (2003).
[31] B. Derrida, Phys. Rev. B **24**, 2613 (1981).
[32] B. Derrida, Phys. Rev. Lett. **45**, 79 (1980).
[33] T. Keyes, Phys. Rev. E **62**, 7905 (2000).
[34] T. Keyes, J. Chowdhary and J. Kim, Phys. Rev. E **66**, 051110 (2002).
[35] M. Sasai, J. Chem. Phys. **118**, 10 651 (2003).
[36] J. D. Bryngelson and P. G. Wolynes, Proc. Natl. Acad. Sci. U.S.A. **84**, 7524 (1987).
[37] J. D. Bryngelson and P. G. Wolynes, J. Phys. Chem. **93**, 6902 (1989).
[38] K. Binder, Comput. Phys. Commun. **122**, 168 (1999).
[39] W. Kauzmann, Chem. Rev. (Washington, D.C.) **43**, 219 (1948).
[40] J. P. K. Doye and D. J. Wales, J. Chem. Phys. **102**, 9659 (1995).
[41] J. P. K. Doye and D. J. Wales, J. Chem. Phys. **116**, 3777 (2002).
[42] F. H. Stillinger, J. Phys. Chem. B **102**, 2807 (1998).
[43] P. G. Debenedetti, F. H. Stillinger, and M. S. Shell, J. Phys. Chem. B **107**, 14434 (2003).
[44] S. Sastry, P. G. Debenedetti, and F. H. Stillinger, Phys. Rev. E **56**, 5533 (1997).
[45] P. G. Debenedetti, T. M. Truskett, C. P. Lewis, and F. H. Stillinger, Adv. Chem. Eng. **28**, 21 (2001).
[46] E. La Nave, S. Mossa, and F. Sciortino, Phys. Rev. Lett. **88**, 225701 (2002).
[47] F. Sciortino, E. La Nave, and P. Tartaglia, Phys. Rev. Lett. **91**, 155701 (2003).
[48] A. Heuer and S. Buchner, J. Phys.: Condens. Matter **12**, 6535 (2000).
[49] C. A. Angell and J. Wong, J. Chem. Phys. **53**, 2053 (1970).
[50] C. A. Angell and K. J. Rao, J. Chem. Phys. **57**, 470 (1972).
[51] C. T. Moynihan and C. A. Angell, J. Non-Cryst. Solids **274**, 131 (2000).
[52] F. H. Stillinger and T. A. Weber, J. Chem. Phys. **83**, 4767 (1985).
[53] P. G. Debenedetti, F. H. Stillinger, T. M. Truskett, and C. J. Roberts, J. Phys. Chem. B **103**, 7390 (1999).
[54] T. M. Truskett and V. Ganesan, J. Chem. Phys. **119**, 1897 (2003).
[55] D. C. Wallace, Phys. Rev. E **56**, 4179 (1997).
[56] P. Shah and C. Chakravarty, J. Chem. Phys. **115**, 8784 (2001).
[57] E. La Nave, F. Sciortino, P. Tartaglia, M. S. Shell, and P. G. Debenedetti, Phys. Rev. E **68**, 032103 (2003).
[58] S. Sastry, Phys. Rev. Lett. **85**, 590 (2000).
[59] C. J. Roberts, P. G. Debenedetti and F. H. Stillinger, J. Phys. Chem. B **103**, 10258 (1999).
[60] R. A. La Violette, J. L. Budzien, and F. H. Stillinger, J. Chem. Phys. **112**, 8072 (2000).
[61] M. Utz, P. G. Debenedetti, and F. H. Stillinger, J. Chem. Phys. **114**, 10049 (2001).
[62] V. K. Shen, P. G. Debenedetti and F. H. Stillinger, J. Phys. Chem. B **106**, 10447 (2002).
[63] C. A. Angell, J. Non-Cryst. Solids **131**, 13 (1991).
[64] G. Ruocco, F. Sciortino, F. Zamponi, C. De Michele, and T. Scopigno, e-print cond-mat/0401449.
[65] F. H. Stillinger, Phys. Rev. E **63**, 011110 (2001).